Energy 96 (2016) 531–544

Contents lists available at ScienceDirect

Energy

journal homepage: www.elsevier.com/locate/energy

Reduction of the generated aero-acoustics noise of a vertical axis wind turbine using CFD (Computational Fluid Dynamics) techniques

M.H. Mohamed [a, b, *]

[a] Mechanical Power Engineering Dept., Faculty of Engineering-Mattaria, Helwan University, P.O. 11718, Cairo, Egypt
[b] Mechanical Engineering Dept., College of Engineering and Islamic Architecture, Umm Al-Qura University, P.O. 5555, Makkah, Saudia Arabia

ARTICLE INFO

Article history:
Received 27 June 2015
Received in revised form
6 December 2015
Accepted 15 December 2015
Available online 4 February 2016

Keywords:
Wind energy
Noise
Acoustics
Double-airfoil
Aerodynamic
CFD (Computational Fluid Dynamics)

ABSTRACT

Noise pollution from wind turbines is an important public health issue, and strict regulations regarding noise levels for nearby residents to a wind farm is a necessity. The fact that more turbines equals higher noise levels constitutes a problem, an expansion of turbines is needed but the nearby residents should not be affected. Noise levels can be measured, but, similar to other environmental attentions, the public's perception of the noise impact of wind turbines is in part a subjective determination. Vertical axis wind turbines are suitable to be established within the densely populated city area. Therefore, the noise item is very important parameter to investigate. In this work, it is introduced an innovative design of the lift VAWTs (vertical axis wind turbines) to reduce the noise emissions. Every blade in the turbine is constructed by two airfoils. The aerodynamics field of the new design have been investigated numerically to obtain the generated noise from new blades. Unsteady Reynolds-averaged Navier–Stokes (URANS) equations are used to obtain the time-accurate solutions. The spacing between the airfoils in every blade at different tip speed ratio has been studied in this work. The results indicated that the 60% spacing is the best configuration of the double-airfoil from the noise reduction point of view. This new design reduces the generated noise by 56.55%

1. Introduction

Wind turbine generators, ranging in size from a few kilowatts to several megawatts, are converting the wind kinetic energy into electricity in wind power stations that involve hundreds of machines. Many installations are in uninhabited areas far from located residences, and therefore there are no visible environmental influences in terms of noise. However, the potential radiated noise can be heard by residents of adjacent neighborhoods, particularly those neighborhoods with low ambient noise levels. The good news is that wind power systems became higher energy efficiency as turbines enlarge substantially their sizes in order to capture more energy from the wind [1]. Manufacturers in wind energy field have improved the know-how, being able to introduce constantly new technology in the quest for efficiency improvement and electricity mass production.

Indeed, wind farms are usually installed based on an accurate or approximated study of the wind resource in a certain area, but the design is always constrained by socio-economic and environmental aspects. It is easy to erect turbines in isolated areas, But vast majority of them are concentrated close to inhabited areas.

Nevertheless, wind turbine noise is a reality, it exists, and its effects can be important depending on the distance between dwellings and turbines, but also depending on wind direction. Wind turbine noise is not as extreme as an aircraft flying over the proximities of an airport, but the source is static and repetitive, emitting noise in a vast range of frequencies. These combined features make wind turbine noise one of the most annoying noise sources for those who are exposed.

In general, noise effects can be classified into three general categories according to a study of Rogers et al. [2]:

- Subjective effects including annoyance and dissatisfaction.
- Disturbance in the human activities such as sleep and hearing.
- Physiological effects such as anxiety or hearing loss.

* Mechanical Power Engineering Dept., Faculty of Engineering-Mattaria, Helwan University, P.O. 11718, Cairo, Egypt. Tel.: +966 597828040; fax: +20 2 2633 2398.
E-mail addresses: moh75202@yahoo.de, mohamed_ibrahim07@m-eng.Helwan.edu.eg, mhmohamed@uqu.edu.sa.

http://dx.doi.org/10.1016/j.energy.2015.12.100
0360-5442/

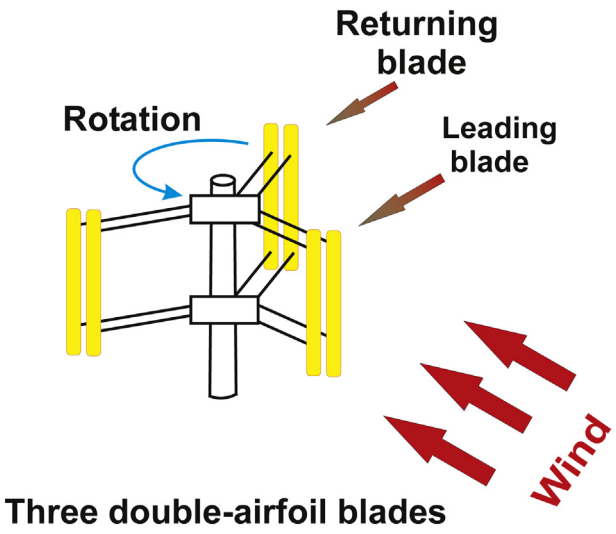

Fig. 1. The new innovative vertical axis Wind turbine.

For those reasons, some European and non-European countries possess regulations regarding industrial noise. Other countries even created specific rules for wind turbine noise [1].

The field of aeroacoustics becomes important in recent years. A considerable development and improvement has been introduced in the aeroacoustics field as any other of the current physics or engineering fields. However, fluid dynamics plays a fundamental role on the aeroacoustics field, trying to model numerous situations involving fluid interaction with solid surfaces. Aeroacoustics is that field of fluid dynamics that studies the origin and propagation of pressure fluctuations generated when a flow interacts with a solid surface. The aeroacoustics along this work are focused on sounds generated by aerodynamic surfaces of the airfoils of the vertical axis wind turbine.

All the types of wind turbines noise frequency range from low values that sometimes inaudible to higher values in the normal audible range [3]. Although, increased distance is advantageous in reducing noise levels, the wind can reinforce noise propagation in certain directions and prevent it in others. At a given sound pressure level, the ear does not sense all frequencies to be of equal loudness. The normal hearing range of the human ear is 20 Hz–20 kHz [4]. Under ideal laboratory conditions, humans can hear sound as low as 12 Hz. Individual hearing range varies according to the general condition of a human's ears and nervous system. The range shrinks during life, usually beginning at around age of eight with the upper frequency limit being reduced. Women typically experience a lesser degree of hearing loss than men, with a later onset. Men have approximately 5–10 dB greater loss in the upper frequencies by age 40 [5].

Wind turbines noise is classified as aerodynamic or mechanical in origin. This work is dealing and assessing the aerodynamics category. Aerodynamic noise components are either narrow-band or broadband and are related closely to the geometry of the rotor, its blades, and their aerodynamic flow environments. The low-frequency, narrow-band rotational components typically take place at the blade passage frequency (the rotational speed times the number of blades) and integer multiples of this frequency [7]. In the next sections, it is presented a novel blade design of vertical axis wind turbine to reduce the turbine aerodynamic noise as shown in Fig. 1. Moreover, a full discussion of the numerical methodology will be introduced to clarify the quantitative and qualitative procedure of the aerodynamic noise calculations.

2. Acoustic pattern

Aerodynamic noise is the main cause of complaint regarding modern wind turbines. Its characteristics can be similar to the ones for regular wind noise and can therefore often be masked by heavy wind.

It is thought that aerodynamic noise from the blades emerges from a number of different mechanisms that are related to the way in which the flow over the airfoil interacts with the surrounding air.

The subsonic flow conditions have five self-noise mechanisms of concern here. At high Reynolds number Re (based on chord length), TBL (turbulent boundary layers) develop over most of the airfoil. Noise is produced as this turbulence passes over the TE (trailing edge). At low Re, largely LBL (laminar boundary layers) develop, whose instabilities result in VS (vortex shedding) and associated noise from the TE. For non-zero angles of attack, the flow can separate near the TE on the suction side of the airfoil to produce TE noise due to the shed turbulent vorticity. At very high angles of attack, the separated flow near the TE gives way to large-scale separation (deep stall) causing the airfoil to radiate low-frequency noise similar to that of a bluff body in flow. Another noise source is vortex shedding occurring in the small separated flow region aft of a blunt TE. The remaining source is due to the formation of the tip vortex, containing highly turbulent flow, occurring near the tips of lifting blades or wings [6].

Prediction techniques of the noise realized by an airfoil are usually based on theoretical principles but use empirically derived components to attain better agreement with what is observed in practice. Previous researches of the reduction of aerodynamic noise from wind turbines has mainly concentrated on the use of serrated trailing edges, different trailing edge and tip shapes, and different airfoil profiles [8]. The wind turbine environmental aspects of noise attach to how it propagates over the terrain surrounding the wind turbine and to how the noise is interpreted by people.

Several standards for calculation of the propagation of the sound are widely used and ranged from basic calculations that assume hemispherical pattern, to complex calculations designed to be done

Table 1
Possible attempts to understand and reduce the aeroacoustics of the wind turbine.

Design modification	Gain	Description and comments
Mathematical model [12] [13],	Acoustics basic model	Stationary wave equation
Extension for Lighthill's analogy [14]	Unbounded flows	Flow interacts with a surface
Arbitrary moving surfaces [16]	FH–W model	Important acoustics model
Experimental research [18] [19], [20] [21],	Measurement improvement	Wind tunnel studies
Optimization of six airfoils [22]	Reduction in aero-acoustics	Numerical computations
Turbulence intensity effect [28]	Sound energy level increases	Flow characteristics
Increasing turbine size [29]	Noise decreases	Turbines design parameter
Rotational speeds [30]	Increasing annoyance	Turbines design parameter
Three-bladed wind turbine [31]	Noisier turbine	Turbine design
VAWT wind turbines [8]	S1046	Turbine airfoil selection

computationally which take into account the influences of terrain shape, barriers, wind speed and direction, atmospheric temperature profile, humidity, and air and ground absorption.

A knowledge of how the sound propagates through the atmosphere is a basic to the process of predicting the noise fields of single and multiple machines. Although much is known about sound propagation in the atmosphere, the least understood factors are the impacts of distance from various types of sources, the effects of such atmospheric factors as absorption in air and refraction caused by sound speed gradients, and terrain effects. In this work, it is introduced a fixed positions of the sound receivers at different locations to capture any sound signals pattern either the hemispherical or not.

3. Purpose of the present work

Studies conducted in Sweden on the leverages of wind power [9,10] detected a correlation between the general attitude of a person towards wind power and their level of annoyance. Pederson [10] found that the most annoying noise heard from wind turbines was a swishing noise, followed by whistling and then pulsating and throbbing noises. Pure wind turbine noise gave very similar annoyance ratings as unmixed highway noise at the same equivalent level, while annoyance by local road traffic noise was significantly higher [11].

3.1. Wind turbine aero-acoustics literatures

All the research and models developed until recent years started from the analogy that Lighthill [12,13], derived from the well-known Navier–Stokes equations. Lighthill proposed a derivation starting from the mass and momentum conservation equations for a flow, up to reaching an acoustic analogy that makes possible to solve the aerodynamic sound by using a stationary wave equation.

Lighthill introduces the concept of a turbulent stress tensor which represents the radiation source terms per unit of volume coming from convection, shear and pressure. Those are modeled using an acoustic quadrupole. Normally the influence of the Lighthill stress tensor focuses on small regions of the flow where perturbations could be introduced by solid surfaces, in the outer regions, any acoustic fluctuation is quickly damped out by the flow convection.

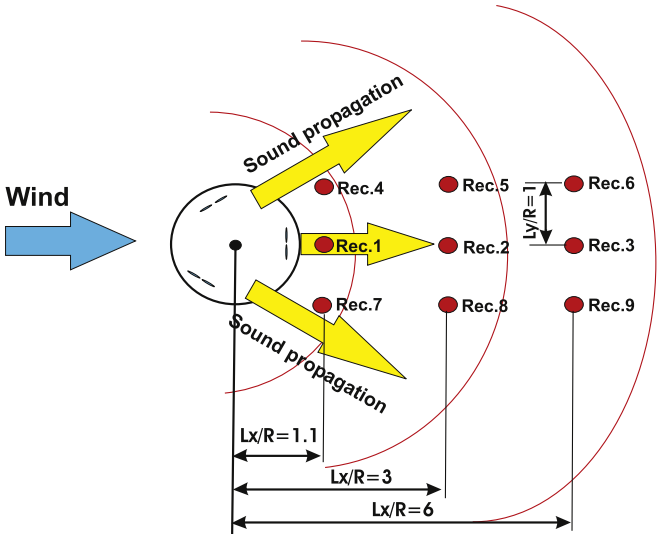

Fig. 3. Pressure wave propagation and the positioning of the receivers.

Kirchhoff reformulated Lighthill's analogy by defining a volume where turbulence fluctuations occur. This formulation, only considers the far field solution as a result of the complexity introduced by retarded time evaluation plus the spatial derivatives. In that sense, the role developed by Lighthill's Tensor becomes clearer although the formulation is only valid when there are no solid boundaries. However, neglecting solid surfaces in the generation of noise, it results in one of the main drawbacks of Lighthill's analogy, being only useful for jet noise.

Curle [14], proposed the first extension for Lighthill's analogy and therefore, expanding Lighthill's assumption for unbounded flows (flow without boundaries). Curle also proved that noise becomes more important when a turbulent flow interacts with a solid surface as a result of the lower Mach numbers and higher Reynolds numbers.

J.E. Ffowcs-Williams, L.H. Hall and D.L. Hawkings, included the influence of arbitrary moving surfaces, also known as FH–W model

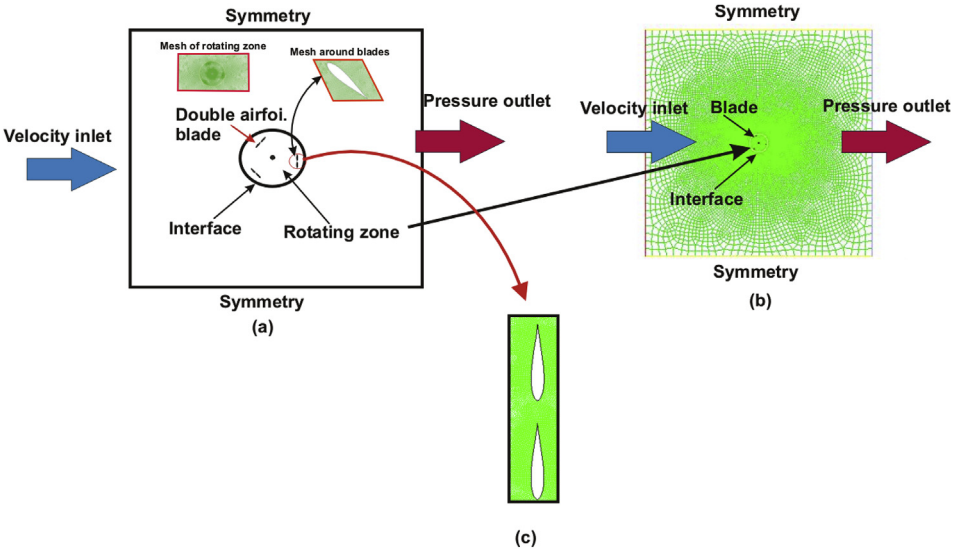

Fig. 2. a) CFD domain and sample of mesh around rotating zone and blade; b) domain mesh; c) mesh around the double-airfoil blade.

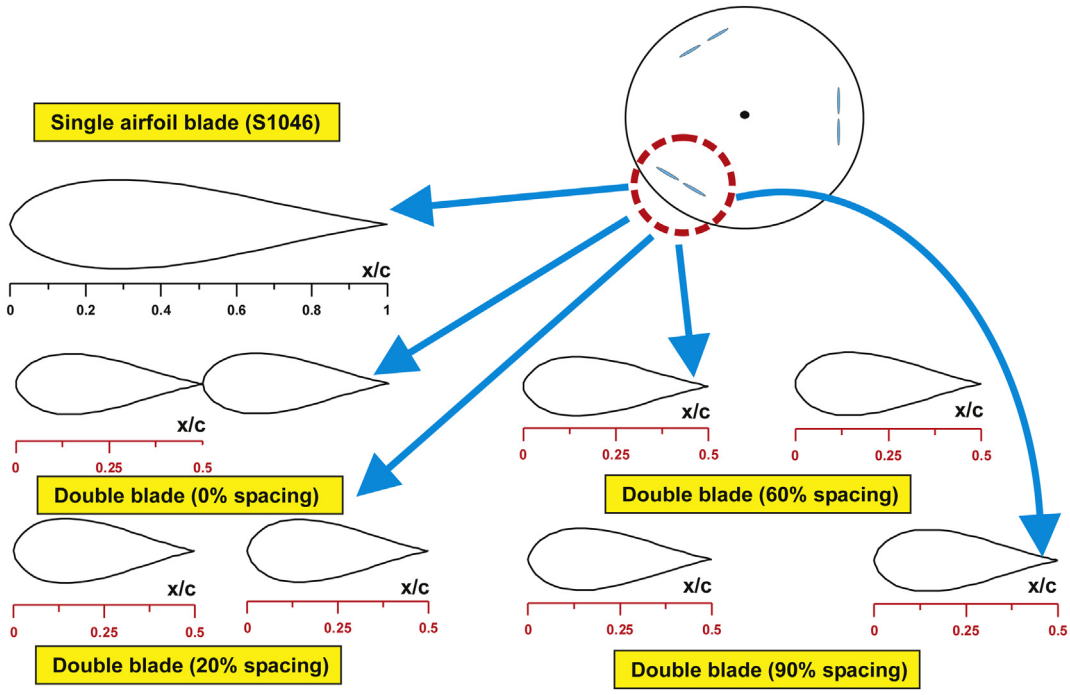

Fig. 4. Different configurations of the double-airfoil blade.

[15] and [16]. The theory is derived similarly from Lighthill's analogy over a scattering half plane. The same quadrupole term (Lighthill's tensor) plus a dipole and monopole distribution result out of it. The conclusion of the FH–W model is that solid surfaces become acoustically equivalent to a distribution of monopoles and dipoles of the solid surface whose strength is equal to the local acceleration of the surface and the net force applied on the fluid respectively. In the common literature, the dipole term is often called loading noise, while the monopole term is well-known as thickness noise.

Amiet [17] proposed a theory for what is called turbulence inflow noise, being the noise radiated for a solid surface as a result of an incoming gust or unsteady flow. In this case, the region of noise radiation is not the trailing edge, but the leading edge. The model was developed for a linearized 3 dimensional flat plate, and it established the basis for most of the turbulence inflow noise models developed afterward. However, the model of Amiet for inflow noise becomes more general, being able to re-express the formulation in order to be applied for a semi-infinite half plane with no leading edge and reproduce the previous formulations for trailing edge noise, i.e. FW–H [15].

Intense experimental research on wind tunnel studies from IAG at University of Stuttgart, [18,19], NREL, NRL [20] and DTU-Ris [21] have been introduced during the last decade, in order to quantify and understand better the coupling effects between aerodynamics and acoustics with the recent improvements in wind tunnel measurement techniques.

Gömena and özerdema focused on the optimization of six airfoils which are widely used on small scale wind turbines in terms of the noise emission and performance criteria and the numerical computations are performed for a typical 10 kW wind turbine. The main purpose of this optimization process was to decrease the noise emission levels while increasing the aerodynamic performance of a small scale wind turbine by adjusting the shape of the airfoil. The results obtained from the numerical analysis of the optimization process have shown that, the considered commercial airfoils for small scale wind turbines are improved in terms of aeroacoustics and aerodynamics. The pressure sides of the baseline airfoils have been manipulated together with the trailing edge and redesigned airfoils have lower levels of noise emission and higher lift to drag ratios [22].

Obviously, noise is an impact factor that must be treated seriously and adequately, but it is only a secondary factor as far as attitudes are concerned. But it is established clear relations between experimental exposure to turbine noise and perceived annoyance [23,24].

Exploration of survey results showed individuals with a more negative attitude to wind turbines perceive more noise from a turbine located close to their dwelling and those perceiving more noise report increased levels of general symptoms. Individuals' personality also affected attitudes to wind turbines, noise perception from small and micro turbines and symptom reporting [25].

Conversely, the noise conspicuous to a listener could actually be increased under certain conditions. For example in the situation where the wind turbine is on a hill and the receptor site is somewhere at the base of the hill screened from the wind, the wind speed on top of the hill is likely to be 1.5:2 times the wind speed at the receptor site. This would reduce the background noise at the receptor site, and the wind turbine noise would thus appear to be more outstanding [26]. Application to a wind park shows clearly the influence of the terrain on the wind velocity and consequently on the SPL (sound pressure level) [27].

Rogers and Omer found that a doubling of the turbulence intensity from 0.3 to 0.6 resulted in an almost doubling of the sound energy level [28].

The results emphasized the hypothesis that the spectrum of wind turbine noise moves down in frequency with increasing turbine size. The relative amount of emitted low-frequency noise is higher for large turbines (2.3:3.6 MW) than for small turbines ($\leq$2 MW). The difference can also be expressed as a downward shift of the spectrum of approximately one third of an octave [29]. At

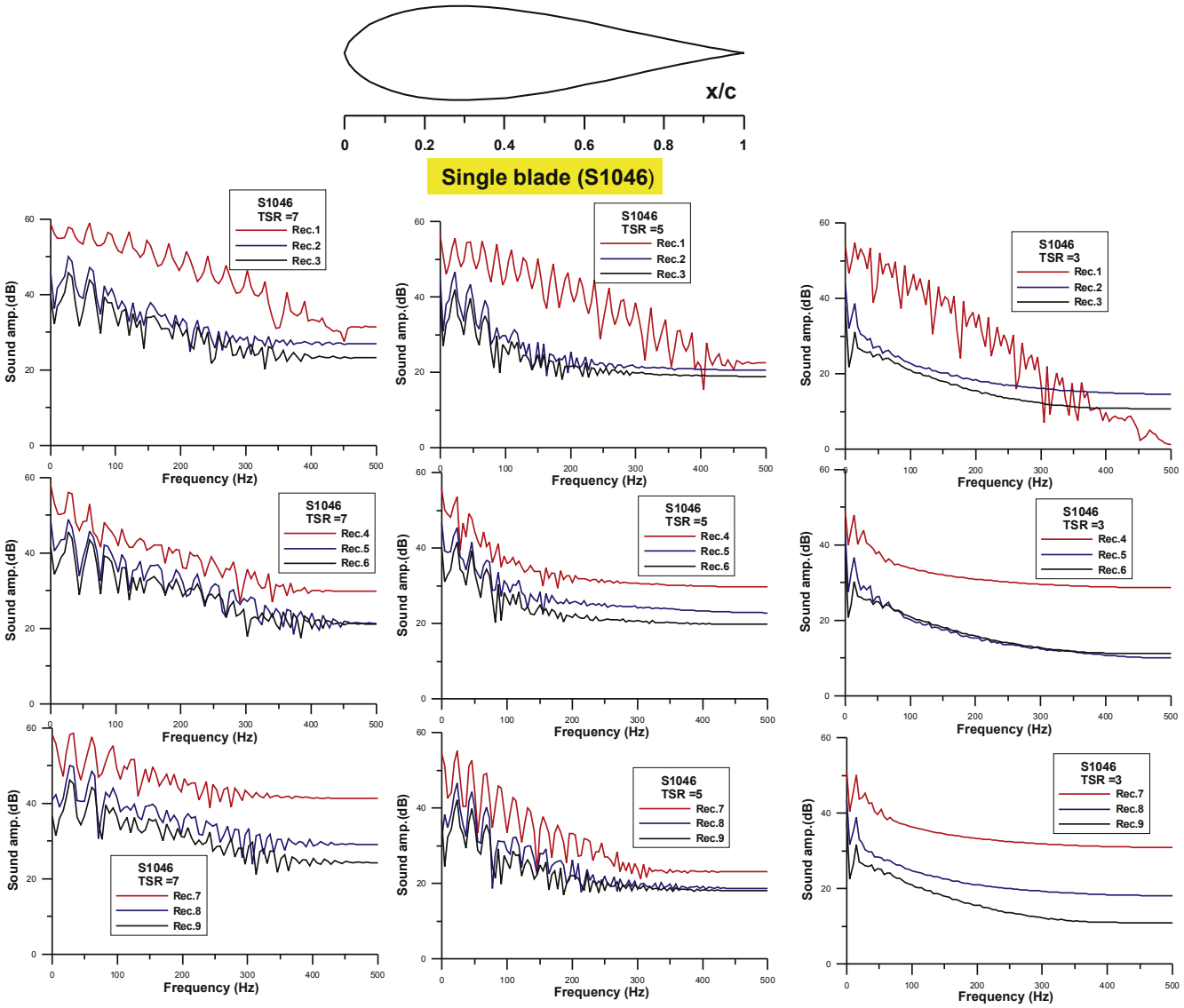

Fig. 5. Generated sound level of the conventional H-rotor consists of S1046 airfoil at different speed ratios.

high rotational speeds the turbines produce a thumping, impulsive sound, increasing annoyance further [30].

Comparison of the noise from the individual blades shows that the tripped blade is significantly noisier than the other two. Narrowband analysis of the de-dopplerized blade noise spectra indicates that trailing edge bluntness noise is not important. All in all, the test results convincingly show that broadband trailing edge noise is the dominant noise source for the three-bladed wind turbine [31]. The most important results concerning such attempts are summarized in Table 1.

3.2. Research gaps and motivations

Because very little information on the acoustics of VAWTs is currently available, it is difficult to directly compare the noise generation characteristics of HAWTs and VAWTs [7]. Only one cited paper [8] has an information about the acoustics of the Vertical axis wind turbine. Mohamed investigated the effect of the blade shape, the speed ratio, solidity and the distance between the noise source (Darrieus turbine) and the receivers.

The author found that the S1046 airfoil is the best airfoil from the noise point of view due to less aerodynamic noise generation. In addition, the results indicated that increasing the tip speed ratio increases the noise generated form Darrieus turbine. Moreover, the decreasing of the solidity reduces the noise emission from the turbine by 7.6 dB if the solidity is reduced from 0.25 to 0.1. Moreover, the average of the noise decay rate is 5.86 dB per every unit distance from the source.

Dumitrescu et al. [32] studied the noise generated from the vertical axis wind turbine but for very low frequency (up to 10 Hz).

There is currently no detailed information available concerning aerodynamic noise sources associated with VAWTs [7]. Thus, to gain an understanding of the acoustics of this type of turbine, additional studies are needed. Therefore, the objectives of this work are (i) to introduce an optimum configuration to reduce the generated aeroacoustics from the vertical axis wind turbine; (ii) to evaluate the CFD ability to accurately predict vertical axis wind turbine noise. Achieving these objectives is important to improve VAWT acceptance, leading to a domestic turbine that could be

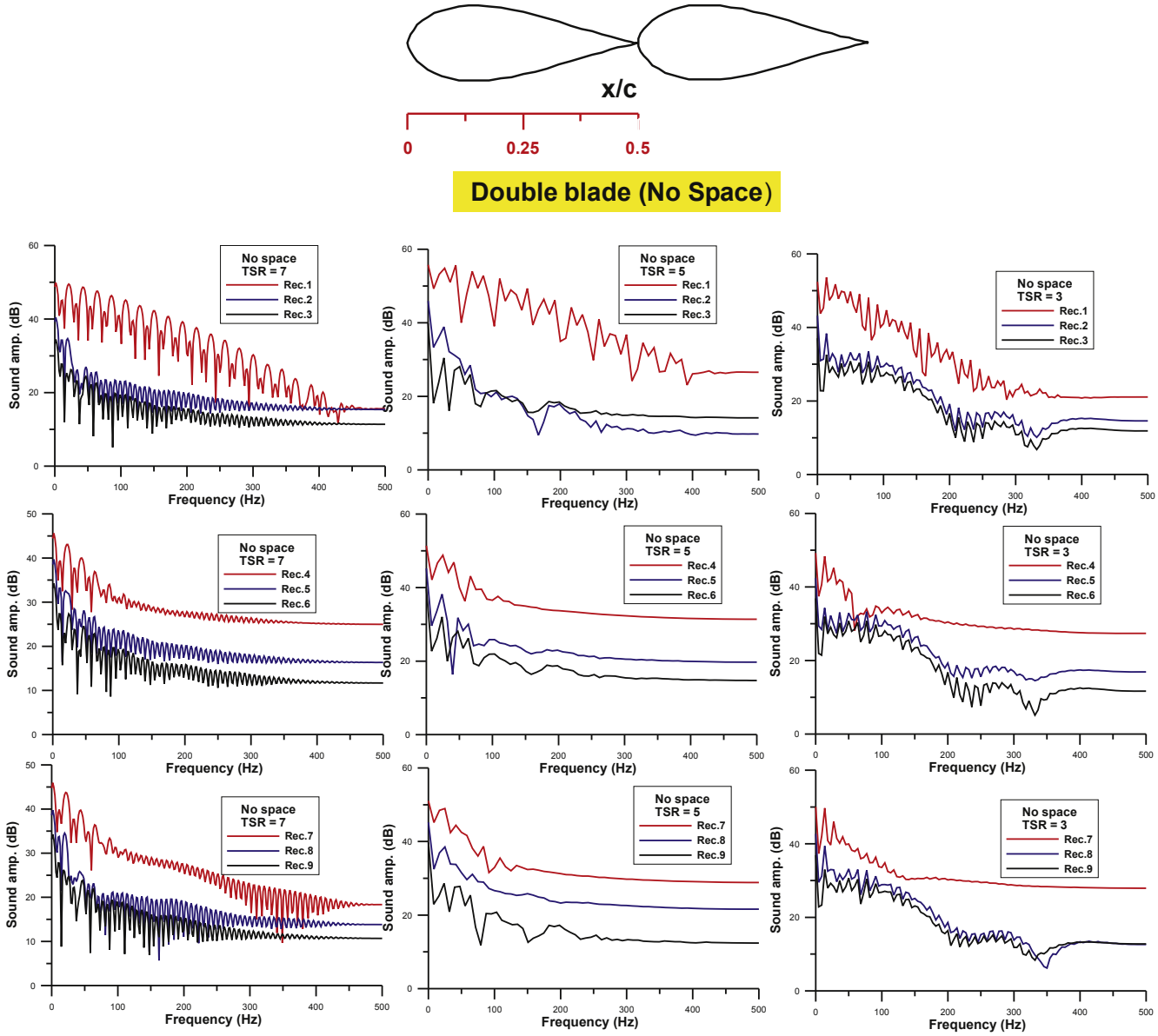

Fig. 6. Generated sound level of the double-airfoil turbine with 0% spacing at different speed ratios.

installed near residential dwellings, since noise would not be a nuisance.

4. Acoustics prediction challenges

The noise from wind turbines at surrounding dwellings is not yet fully investigated with respect to noise level distribution, directivity or subjective experience. In this paper, the integral method based on acoustic analogy has been used because it is applicable only to predicting the propagation of sound toward open areas.

Basically, the problem is based on solving fluctuations in pressure at a given location, and this raises some further problems. CFD techniques have been evolved quite rapidly in previous decades. Computers evolution ables to perform high number of calculations. However, the problem is still the same; the higher number of points in a fluid domain, the better the solution is approximated. At the same time, more computational times are required either to solve the vast amount of grid points for a steady state simulation or to preserve the stability of a transient scheme, defined by the Courant number.

The main challenge in numerically predicting sound waves repels from the well-recognized fact that sounds have much lower energy than fluid flows, typically by several orders of magnitude. This poses a great challenge to the computation of sounds in terms of difficulty of numerically resolving sound waves, especially when one is interested in predicting sound propagation to the far field. Another challenge takes place from the difficulty of predicting the turbulence flow phenomena in the near field that are responsible for generating sounds. The accurate solution of the noise problem is strongly influenced by the unsteadiness of the rotor flow field, the nonuniform inflow effects and the blade aerodynamic parameters which are included in the numerical model [33].

4.1. Ffowcs Williams and Hawkings (FW–H) equations

Lighthill [12] established the basis of aeroacoustics theory. In order to understand other models presented in the manuscript, it is

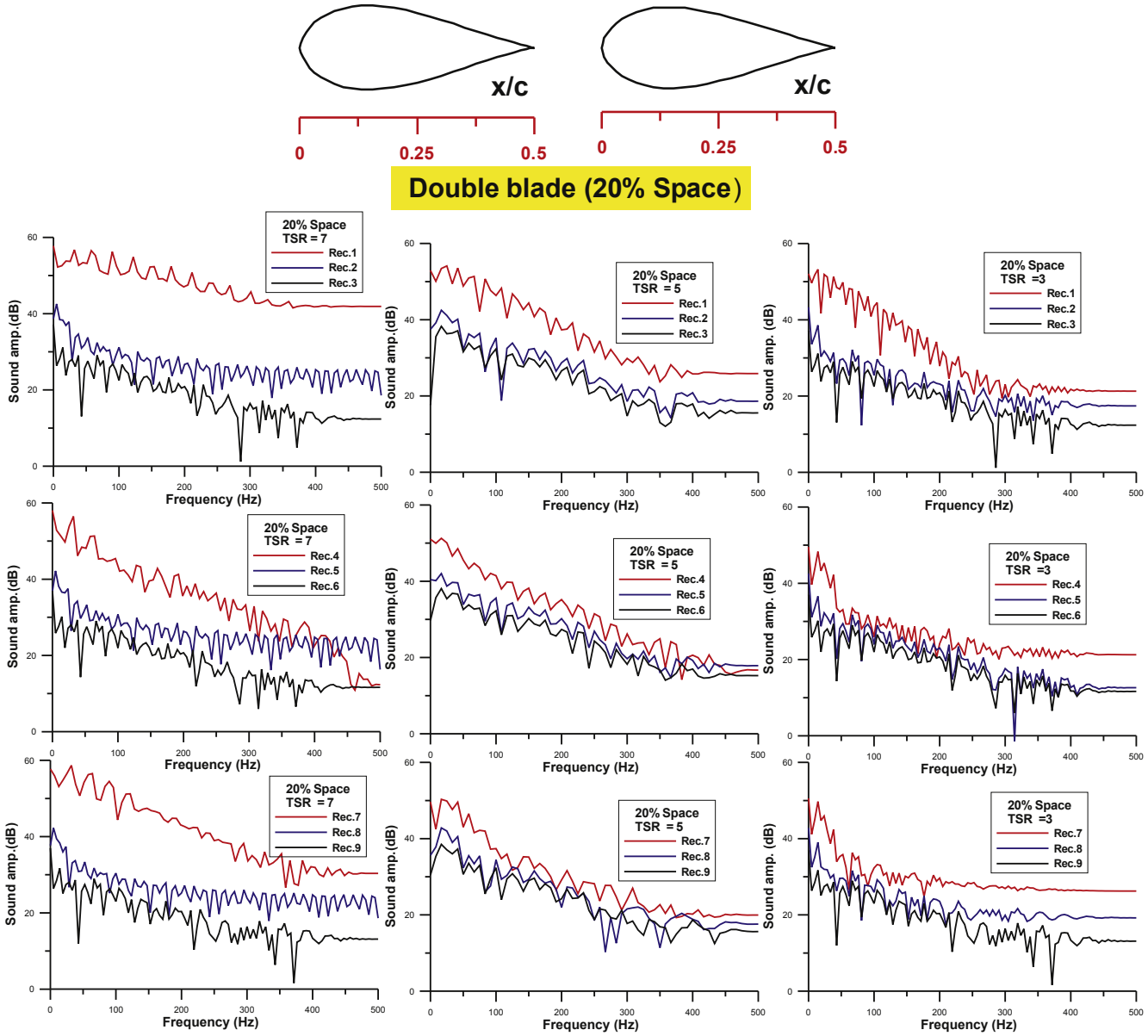

Fig. 7. Generated sound level of the double-airfoil turbine with 20% spacing at different speed ratios.

interesting to show the basic hypotheses behind his analogy for an inhomogeneous and unbounded flow. Lighthill's analogy is derived from the well-known Navier–Stokes equations of mass and momentum conservation respectively.

Lighthill's equations, describe the motion of a wave moving at a speed of propagation in a domain at rest as a result of external fluctuations introduced by the stress tensor. Lighthill's stress tensor, τ_{ij}, is the forcing term, being the mathematical modeling of sound generation. Effects of flow convection, shear stress and acoustic propagation constitute this term. In most of the cases, the meaningful term in Lighthill's stress is convection, especially if Reynolds numbers are high enough. The physical explanation behind Lighthill's stress tensor is formulated on a force exerted by a distribution of quadrupoles bouncing stretching and squeezing each other in different configurations. Their instantaneous intensity per unit of volume is equal to the local stress.

Ffowcs-Williams, Hall [12], and Hawkings [13] extended Lighthill's formulation by applying the same analogy on a domain split in two parts; the surrounding flow and the moving surfaces. In that sense, this theory couples perfectly the acoustic radiation of an arbitrary moving surface within the flow in which is immersed. By means of this model, several applications can be analyzed, such as helicopter wings, wind turbine blade, propellers and turbofans.

The FW–H formulation espouses the most general form of Lighthill's acoustic analogy [12], and is capable of predicting sound generated by equivalent acoustic sources, for instance, vertical axis wind turbine. Time-accurate solutions of the flow-field variables around the turbine, such as pressure, velocity components, and density on source surfaces, are required to evaluate the surface integrals. Time-accurate solutions can be obtained from unsteady Reynolds-averaged Navier–Stokes (URANS) equations. The FW–H acoustics model in FLUENT permits you to select multiple source surfaces and receivers. Sound pressure signals can be processed using the FFT (fast Fourier transform) and associated postprocessing capabilities to compute and plot all acoustic quantities [34].

The Ffowcs Williams and Hawkings (FW–H) equation is basically an inhomogeneous wave equation that can be obtained by manipulating the continuity equation and the

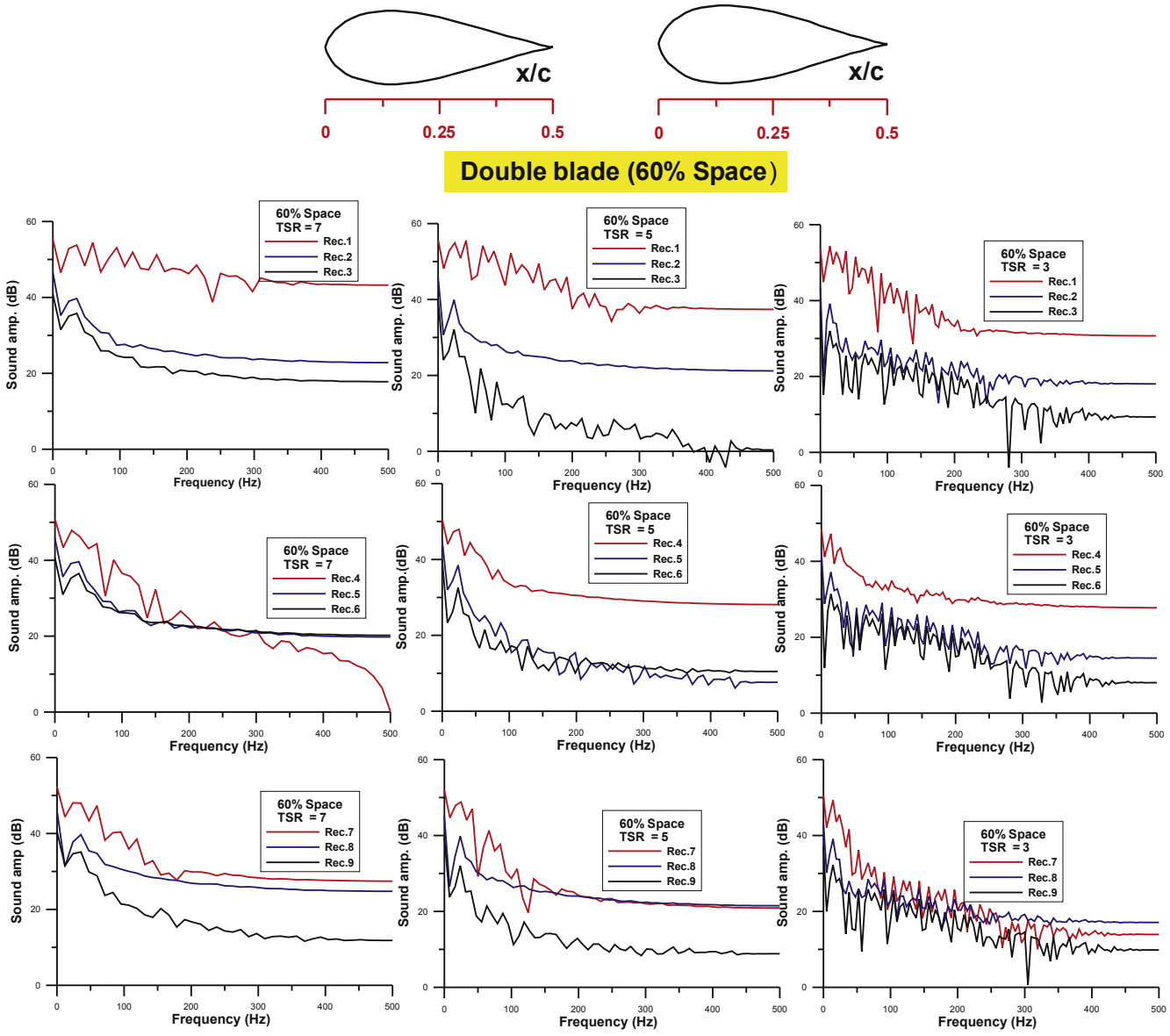

Fig. 8. Generated sound level of the double-airfoil turbine with 60% spacing at different speed ratios.

Navier–Stokes equations. The FW–H [15,34,35] equation can be written as:

$$\frac{1}{a_o^2}\frac{\partial^2 \acute{p}}{\partial t^2} - \nabla^2 \acute{p} = \frac{\partial^2}{\partial x_i \partial x_j}\{T_{ij}H(f)\} - \frac{\partial}{\partial x_i}\{[P_{ij}n_j + \rho u_i(u_n - v_n)]\delta(f)\} + \frac{\partial}{\partial t}\{[\rho_o v_n + \rho(u_n - v_n)]\delta(f)\} \quad (1)$$

where u_i = fluid velocity component in the x_i direction
u_n = fluid velocity component normal to the surface f = 0
v_i = surface velocity components in the x_i direction
v_n = surface velocity component normal to the surface
$\delta(f)$ = Dirac delta function
H(f) = Heaviside function
p = The sound pressure at the far field
T_{ij} = The Lighthill's stress tensor

$\acute{p}$ is the sound pressure at the far field ($\acute{p} = p - p_0$). $f = 0$ denotes a mathematical surface introduced to "embed" the exterior flow problem ($f > 0$) in an unbounded space, which facilitates the use of generalized function theory and the free-space Green function to obtain the solution. The surface ($f = 0$) corresponds to the source (emission) surface (blades and shaft). n_i is the unit normal vector pointing toward the exterior region ($f > 0$), a_0 is the far-field sound speed, and T_{ij} is the Lighthill's stress tensor [34], defined as

$$T_{ij} = \rho u_i u_j + P_{ij} - a_o^2(\rho - \rho_o)\delta_{ij} \quad (2)$$

P_{ij} is the compressive stress tensor. For a Newtonian fluid, this is given by

$$P_{ij} = p\delta_{ij} - \mu\left[\frac{\partial u_i}{\partial x_j} + \frac{\partial u_j}{\partial x_i} - \frac{2}{3}\frac{\partial u_k}{\partial x_k}\delta_{ij}\right] \quad (3)$$

Free-stream quantities are denoted by the subscript o. The distribution of dipoles is known as TN (Thickness Noise), representing the

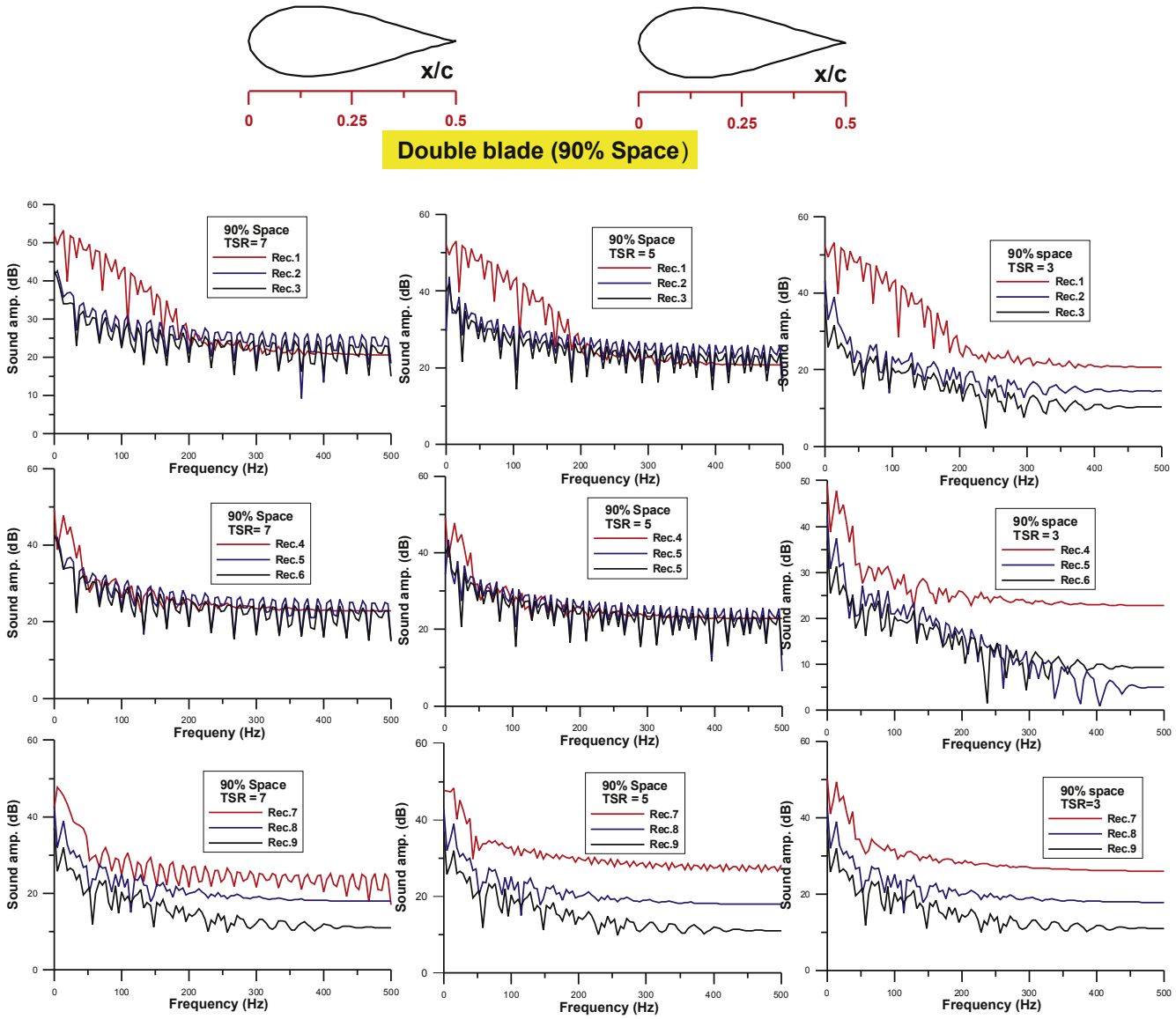

Fig. 9. Generated sound level of the double-airfoil turbine with 90% spacing at different speed ratios.

displacement of a fluid as a result of a moving sound source. On the other hand, the distribution of monopoles is known as LN (Loading Noise) representing the force introduced on the fluid resulting from the acceleration of the moving surface. In details, TN (Thickness noise) is dependent only on the shape and motion of the blade, and can be thought of as being caused by the displacement of the air by the rotor blades. It is primarily directed in the plane of the rotor. Loading noise is an aerodynamic adverse effect due to the acceleration of the force distribution on the air around the rotor blade due to the blade passing through it, and is directed primarily below the rotor. In general, loading noise can include numerous types of blade loading: some special sources of loading noise are identified separately. Changes in blade-section motion relative to the observer as the steadily loaded propeller rotates, generally referred to as "loading" noise. This source tends to dominate at low blade speed.

The solution to Eq. (1) is obtained using the free-space Green function $(\delta(g)/4\pi r)$. The whole solution consists of surface integrals and volume integrals. The surface integrals explain the contributions from monopole and dipole acoustic sources and partially from quadrupole sources, whereas the volume integrals represent quadrupole (volume) sources in the region outside the source surface. The contribution of the volume integrals becomes small when the flow is low subsonic as in the Darrieus turbine case. In FLUENT, the volume integrals are converted to surface fluxes [34]. Thus, we have

$$\acute{p}(\vec{x},t) = \acute{p}_T(\vec{x},t) + \acute{p}_L(\vec{x},t) \tag{4}$$

where

$$4\pi\acute{p}_T(\vec{x},t) = \int_{f=0} \left[\frac{\rho_o\left(\dot{U}_n + U_{\dot{n}}\right)}{r(1-M_r)^2}\right] ds + \int_{f=0} \left[\frac{\rho_o U_n\{r\dot{M}_r + a_o(M_r - M^2)\}}{r^2(1-M_r)^3}\right] ds \tag{5}$$

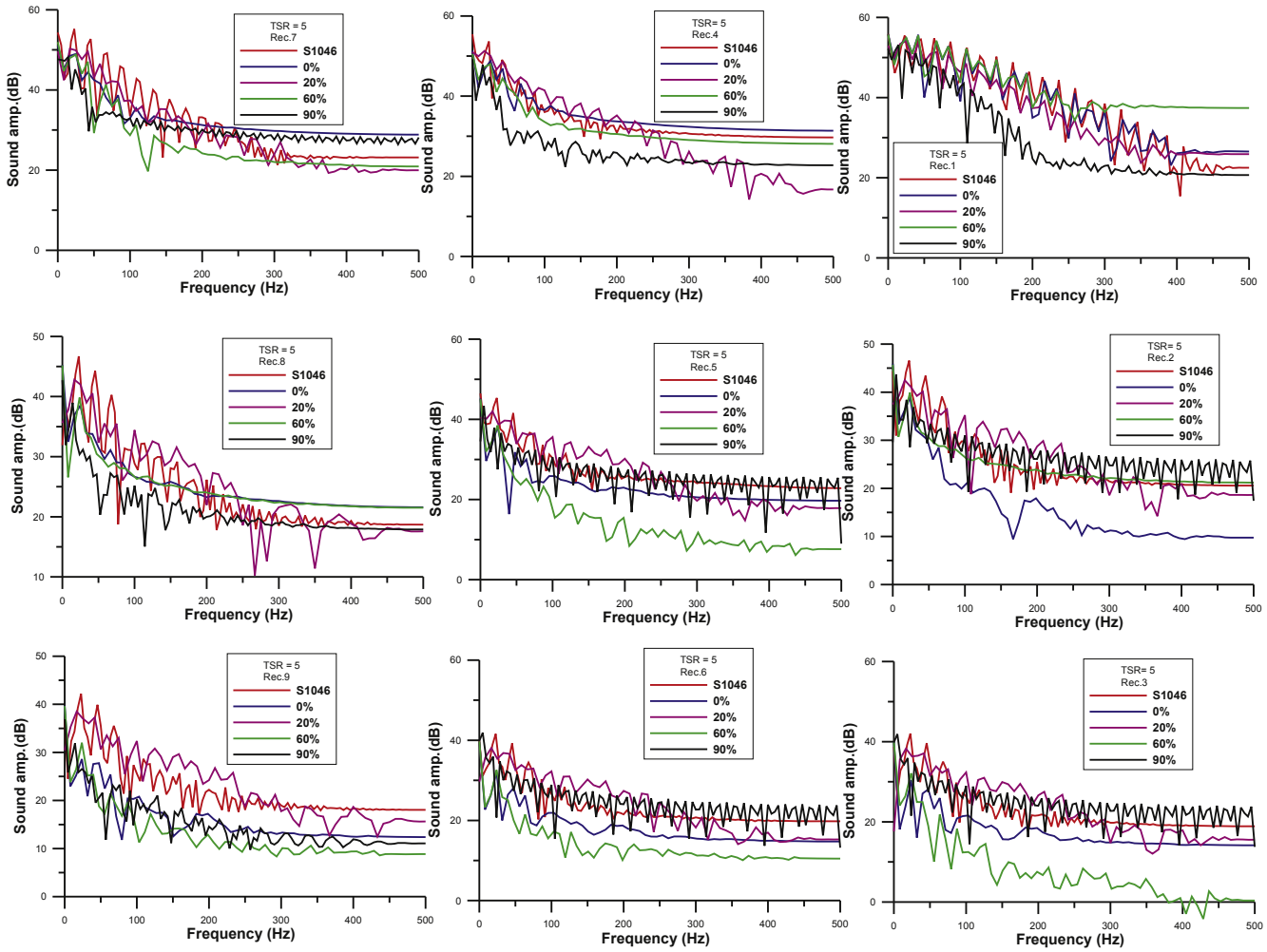

Fig. 10. Sound generation comparison between the different configurations of the double-airfoil turbine and the conventional S1046 H-rotor.

$$4\pi p_L'(\vec{x},t) = \frac{1}{a_o}\int_{f=0}\left[\frac{\dot{L_r}}{r(1-M_r)^2}\right]ds + \int_{f=0}\left[\frac{L_r - L_M}{r^2(1-M_r)^2}\right]ds + \frac{1}{a_o}\int_{f=0}\left[\frac{L_r\left\{r\dot{M}_r + a_o\left(M_r - M^2\right)\right\}}{r^2(1-M_r)^3}\right]ds \quad (6)$$

where

$$U_i = v_i + \frac{\rho}{\rho_o}(u_i - v_i) \quad (7)$$

$$L_i = P_{ij}\hat{n}_j + \rho u_i(u_n - v_n) \quad (8)$$

When the integration surface synchronizes with an impenetrable wall, the two terms on the right in Eq. (4), $p_T'(\vec{x},t)$ and $p_L'(\vec{x},t)$, are often pointed out to as thickness and loading terms, respectively, in light of their physical meanings. The square brackets in Eqs. (5) and (6) mention that the kernels of the integrals are computed at the corresponding retarded times, τ, defined as follows, given the observer time, t, and the distance to the observer, r,

$$\tau = t - \frac{r}{a_o} \quad (9)$$

The various subscripted quantities appearing in Eqs. (5) and (6) are the inner products of a vector and a unit vector tacit by the subscript. For instance, $L_r = \vec{L}\cdot\vec{r} = L_i r_i$ and $U_n = \vec{U}\cdot\vec{n} = U_i n_i$, where $\vec{r}$ and $\vec{n}$ denote the unit vectors in the radiation and wall-normal directions, respectively. The dot over a variable announces source-time differentiation of that variable [34]. There are some remarks regarding the applicability of this integral solution:

(1) The FW–H formulation can treat rotating surfaces as well as stationary surfaces.
(2) It is not required that the surface $f = 0$ coincide with body surfaces or walls. The formulation allows source surfaces to be permeable, and therefore can be placed in the interior of the flow.
(3) When a permeable source surface (either interior or non-conformal sliding interface) is placed at a certain distance of the body surface, the integral solutions given by Eqs. (5) and (6) involve the contributions from the quadrupole sources within the region enclosed by the source surface. When using a permeable source surface, the mesh resolution needs to be fine enough to resolve the transient flow structures inside the volume enclosed by the permeable surface.

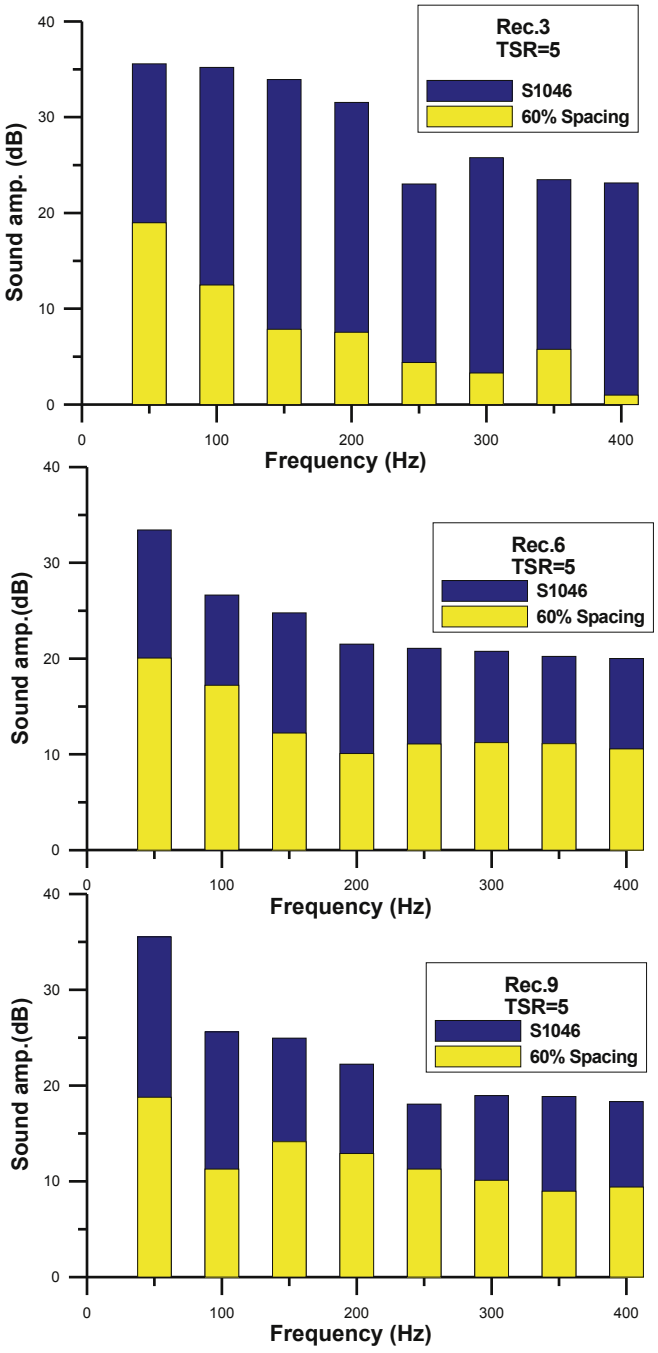

Fig. 11. Optimal configuration (60% spacing) sound level compared with the conventional S1046 vertical axis wind turbine.

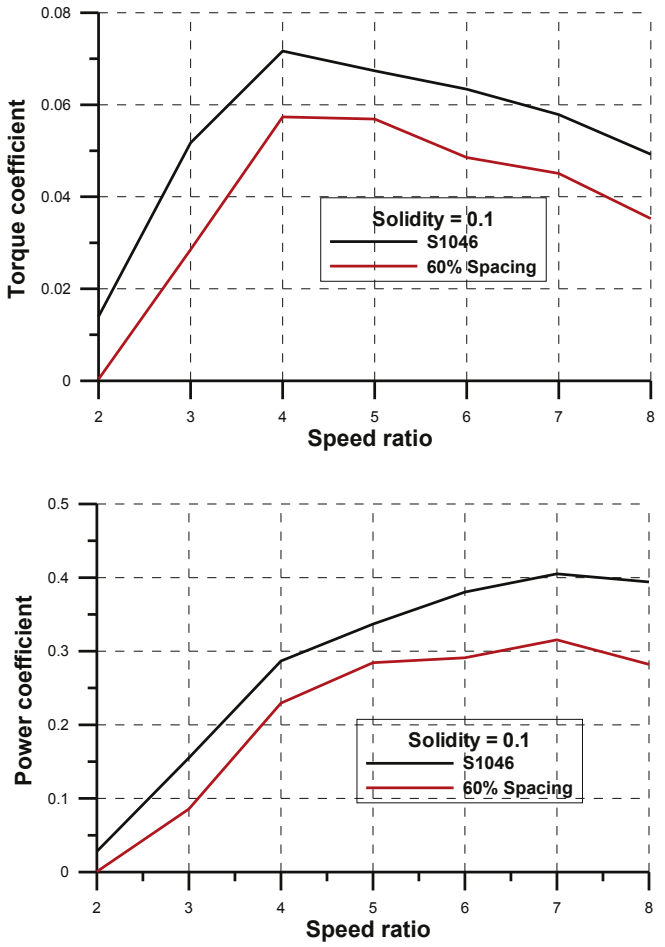

Fig. 12. Performance of optimal configuration (60% spacing) compared with the conventional turbine performance.

The previous theory can be applied for multiple problems involving moving surfaces. However, when it is applied on airfoils, this one is modeled as a semi-infinite half scattering plate, being the trailing edge the discontinuity point between the surface and near wake flow that introduces noise radiation.

5. CFD (Computational Fluid Dynamics) methodology

From the above considerations, it is clear that the development of a methodology that predicts in considerable detail and with sufficient accuracy the entire flow field of a flow and, in particular, unsteady flow around turbines is highly desirable. Such a methodology exists in form of CFD (computational fluid dynamics). CFD is the analysis of engineering systems involving fluid flow, heat transfer and associated phenomena, such as two-phase flow, by means of computer-based simulation.

Due to the highly time-dependent nature of the flow around the vertical axis wind turbines, the CFD simulation of these turbines is a very difficult mission. It is therefore necessary to check the full numerical model with great care. Thereafter, the resulting methodology must be validated. ANSYS-Fluent has been used in this work. Unsteady Reynolds-Averaged Navier–Stokes equations have been solved using the SIMPLE algorithm for pressure–velocity coupling. The Finite-Volume method has been used as a Discretization procedure with second-order upwind scheme for all variables. Fig. 2 illustrates all the details about the boundary conditions and the computational domain. The author validated this model and CFD procedure in previous work [36,37]. The validation comparison has been conducted between the present model results and published experimental and CFD results for a H-rotor Darrieus turbine [36,37]. The results indicated that an acceptable agreement between the experiments and present CFD. The power coefficient (C_p) (turbine efficiency) is investigated quantitatively and qualitatively by using the realizable k-ε turbulence model. The realizable k-ε model is recommended for rotating bodies [34]. Therefore, in this work the realizable k-ε turbulence model will be retained in all the aerodynamic simulation. Similar trend has been observed in other studies encompassing rotating blades [38,39] and airfoils as

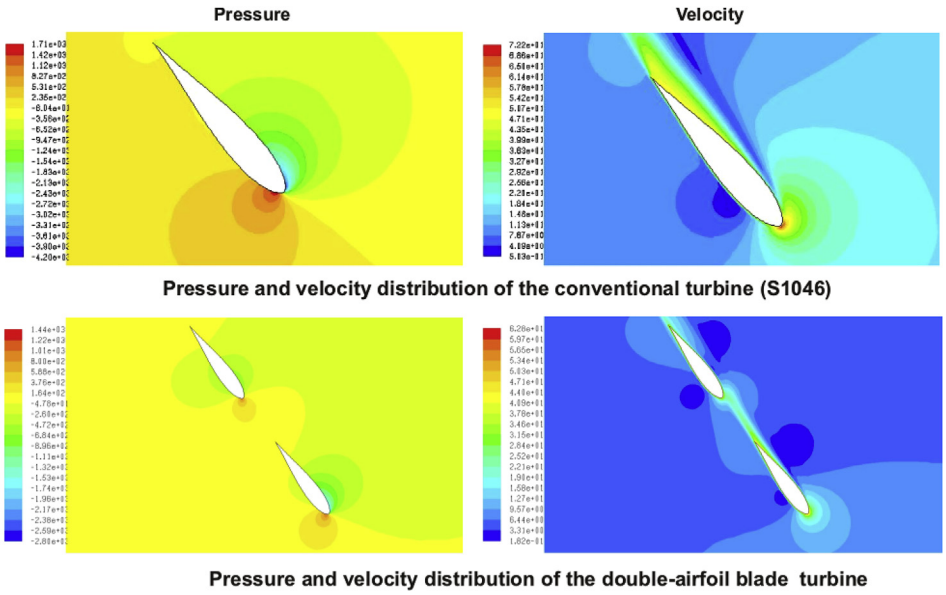

Fig. 13. Pressure and velocity distribution around the optimum design (60% spacing) and the conventional turbine (S1046).

in Refs. [40,41], proving the interest of the realizable k-model for fast CFD simulations. The SMM (Sliding Mesh Model) is used to solve The unsteady flow. The sliding mesh model is the most accurate method for simulating flows in multiple moving reference frames, but also the most computationally demanding. The sliding mesh model allows adjacent grids to slide relative to one another by making a link between the stationary and rotating zone interfaces. In doing so, the grid faces do not need to be aligned on the grid interface. This situation requires a means of computing the flux across the two non-conformal interface zones of each grid interface. To compute the interface flux, the intersection between the interface zones is determined at each new time step. The resulting intersection produces one interior zone (a zone with fluid cells on both sides). Five complete revolutions are always computed by constant time step equals 0.001. the time step independence has been checked to reduce the solution error. The time step size was equivalent to one degree of turbine rotation; this corresponds to time step 0.001 s. The CFL equals 0.245. However, Trivellato and Castelli, (2014) [42], added a more restrictive value for CFL less than 0.15 as compared with the literature criterion. Actually, The Trivellato and Castelli restriction prompts a dramatic increase of CPU times. This findings will hopefully give some guidance to choose meaningful angular marching steps of rotating grids.

The flow properties are calculated by averaging the results during the last four revolutions. The acoustic signals for all receivers (see Fig. 3) can be obtained and captured during instantaneously during the last revolution. The boundary conditions can be summarized as: the inlet velocity is retained as constant and equals 9 m/s and the pressure outlet is the atmospheric pressure (see Fig. 2).

Five revolutions for one specific configuration takes about 360 mins of computing time on the standard PC. A mesh size independence test is accomplished for one geometrical configuration. Several different two-dimensional, unstructured grids of increasing density and quality, collected of different mesh size ranging from 6000 up to 135,000 cells are scanned.

This test introduces more than 80,000 cells lead to a relative variation of the output quantity below 1.124%. The moderate grid range between 80,000 and 100,000 cells has been conserved for all further results due to the computing time. The adequate size of the computational domain has been studied [36].

6. Results and discussion

The aerodynamic noise associated with vertical axis wind turbines is very rare. It is recommended in Refs. [36,37] a design for Darrieus turbine consists of S1046 airfoils cross section. The coordinates of this airfoil can be obtained from Ref. [43]. In the same sequence, in Ref. [8] it is presented an information about the acoustics of the vertical axis wind turbine. This research investigated the effect some parameters on the generated noise from the vertical axis wind turbine (Darrieus turbine). The author found that the best airfoil is S1046 from the high performance, wider operating range (beyond $\lambda = 8$) and low noise point of views. In this work, a double-airfoil blade (Fig. 1) is introduced as a novel idea to reduce the noise from this vertical axis wind turbine. In Ref. [32] the authors studied the VAWTs acoustics in low frequency range (up to 10 Hz), however, in this work, the frequency range is increased up to 500 Hz.

6.1. Speed ratio effect

Firstly, the impact of the tip speed ratio has been studied. The tip-speed ratio (λ) is a dimensionless number which can be defined as ($\lambda = \omega R/U$), where R is the rotor radius (m), ω is the rotating speed (rad/s) and U is the flow velocity (m/s). Here, the double-airfoil blade is used with different spacing 0%, 20%, 60% and 90% as shown in Fig. 4. Both the airfoils are the same profile of S1046 and constant solidity equals 0.1 and the chord (c) is divided by equal ratio between the two airfoils. The constant solidity ($\sigma = 0.1$) is very important issue in the calculation of the aeroacoustics as well as the aerodynamic performance, this is due the strong effect of the solidity on the pressure difference across the blades.

According to [36,37], increasing the solidity reduces the operating range of the turbine. Moreover, the increasing of the solidity increases the pressure fluctuations downstream the rotor, this means the turbine will be noisier than low solidity turbine and it is not recommended in the residential areas. Nine receivers are used to collect the noise signals under different working conditions as shown in Fig. 3. The results indicate that the increasing of the speed ratio increases slightly the noise form vertical axis wind turbine as shown in Fig. 5, Fig. 6, Fig. 7, Fig. 8 and Fig. 9. Three different speed

ratios have been studied ($\lambda = 3$, $\lambda = 5$ and $\lambda = 7$) for the same turbine solidity ($\sigma = 0.1$) and for all different spacing configurations of the double-airfoil turbine. The operating range of the lift vertical axis wind turbine is between 2 and 8. Therefore, the selection of 3, 5 and 7 speed ratios is to cover the operating rang of this types of the wind turbines. The results indicate to a logic reduction of the noise level with the increase distance between the receivers and the sound source. For all receivers, the results suggested that the rotational speed should be small to reduce the noise generations. The average reduction of the sound amplitude is 15.5 dB, if the speed ratio decreases from $\lambda = 7$ to $\lambda = 3$. However, to obtain the best performance (maximum efficiency), the turbine should rotate with speed ratio around 5, this means the reduction of the noise is equal 7.8 dB. This reduction is a significant number especially in the residential areas.

6.2. Double-airfoil spacing effect

The present work targeted to reduce the noise generated from the vertical axis wind turbine by changing the design of the blade. The new blade consists of two airfoils of S1046 section. The selection of S1046 airfoil section is due to the previous work of the author [36]. In Refs. [36], it is studied the effect of the airfoil shape on the characteristics performance of the rotor. The results of this research indicated that the S1046 is the best airfoil from the performance point of view. Furthermore, in 2014 [8], the author found that S1046 is lower noise generation with the comparison with different common airfoils. In this work, it is used the same airfoil (S1046), but the chord is divided into two equal parts. This means, every blade consists of two airfoils with S1046 profile as shown in Figs. 1 and 4. Nevertheless, the solidity $\sigma = nc/2R$ will be kept constant for all the spacing between the two airfoils and equals 0.1. This solidity ($\sigma = 0.1$) is the lowest noise generation than the other solidities as discussed in Ref. [8]. The author believes that the spacing between the two airfoils is affecting on the noise generated from the blades. Therefore, the results in Fig. 10 introduce the effect of the spacing between the blade airfoils. From the results, it has been concluded that the spacing between airfoils is very effective on the generated noise level as shown in Fig. 10. Due to the comparison with the single airfoil turbine (conventional design consists of S1046 airfoil), the new design with double-airfoil with 60% spacing is the best configuration. Most of the receivers introduce the same result that the 60% is better than the conventional vertical axis wind turbine consists of S1046 for all frequencies. The new configuration reduces the average sound level by 56.55% with comparison to the conventional turbine (S1046) as shown in Fig. 11. This average sound level is calculated at last set of receivers at $L_x/R = 6$ (receiver 3, receiver 6 and receiver 9). The results are relatively encouraging, since the new rotor (double-airfoil blade) induces minimal values of the sound level much lower than those obtained with the conventional rotor (S1046 cross section). Nevertheless, it also introduces low values of the torque and power coefficient as shown in Fig. 12. Overall, the mean value of the torque and power coefficients is decreased by 6.8% less than the conventional rotor. The static pressure and the velocity distributions around the 60% spacing double airfoil blade are shown in Fig. 13 compared with the pressure and velocity distributions around the conventional turbine blade, showing the stall and separation on the blades. As mentioned before, circular wave fronts propagate in all directions from a point source or multiple source. For the optimum configuration (60% spacing), the sound levels decay at the rate of 3.74 dB per unit of distance of the receiver from the source (L_x/R) at frequency 200 Hz. It is noted that the average decay rate is approximately constant. From this reduction rate, noise radiation vanishing distance ratio (L_x/R) is calculated as 10.1. This means, the effect of the noise disappears completely after a distance equals ten times the turbine radius. Therefore, it is recommended the double-airfoil blade for the vertical axis wind turbines from the point of view of the less noise generation.

7. Conclusions

VAWTs (Vertical Axis Wind Turbines) appear to be particularly promising for the conditions of low wind speed and the residential zones. Currently, the available information about the aerodynamic noise is rare, in particular, for the vertical axis wind turbine. An innovative design of the vertical axis wind turbine is introduced in this work to reduce the generated aeroacoustics. The new turbine is constructed of three blades, every blade consists of double airfoils. S1046 is the profile which used for the every airfoil in the new blade design. The Ffowcs Williams and Hawkings (FW−H) equations are used in this work to calculate the generated aeroacoustic from the new vertical axis wind turbine. The effect of spacing between the double airfoils and the speed ratio as well as the distance between the noise source (turbine blades) and the receivers are investigated in this paper. The results indicated that increasing the tip speed ratio increases slightly the noise generated by the lift vertical axis wind turbine either for the standard shape or the double-airfoil blade. Additionally, increasing the distance between the airfoils in the double-airfoil configuration to certain value decreases the noise emission from the new turbine for the same solidity $\sigma = 0.1$. Most of the receivers indicated that the 60% spacing is the best configuration to reduce the noise from this wind turbine type (vertical axis wind turbine with double-airfoil blades). Moreover, the comparison between the conventional H-rotor and the new design (optimum configuration) introduces an impressive result that the new configuration reduces the average sound level by 56.55%. Nevertheless, this optimum design reduce the power and torque coefficient by 6.8%. Finally, it is concluded that this work is unique from the point of views of the design and the reduction of the noise emissions field, in particular, for vertical axis wind turbine.

Acknowledgments

The author would like to thank Prof. Dominique Thévenin the head of Laboratory of Fluid Dynamics and Technical Flows University of Magdeburg “Otto von Guericke” Magdeburg, Germany, for his help. Moreover, the effort of the Dip-Ing. L. Daróczy is appreciated.

References

[1] Oriol Ferret Gasch. Assessment, development and validation of wind turbine rotor noise prediction codes. European Wind Energy Master-EWEM, DTU; 2014.
[2] Rogers AL, Manwell JF, Wright S. Wind turbine acoustic noise. Technical report. Renewable Energy Research Laboratory, University of Massachusetts; 2002.
[3] Kelley ND, McKenna HE, Hemphill RR, Etter CL, Garrelts RC, Linn NC. Acoustic noise associated with the MOD-1 wind turbine: Its source, impact and control. SERI TR-635−1166. Golden, Colorado: Solar Energy Research Institute; Feb. 1985.
[4] Robinson D, Dadson R. A re-determination of equal loudness relations for pure tones. Br J Appl Acoust 1956;7:166−81.
[5] Rossing Thomas. Springer handbook of acoustics. Springer; 2007. ISBN 978−0387304465.
[6] Brooks Thomas F, Stuart Pope D, Marcolini Michael A. Airfoil self-noise and prediction. NASA Reference Publication, 1218. 1989.
[7] Hubbard HH, Shepherd KP. Wind turbine acoustics. NASA Technical Paper 3057 DOE/NASA/20320−77. 1990.
[8] Mohamed MH. Aero-acoustics noise evaluation of H-rotor Darrieus wind turbines. Energy 2014;65:596−604.
[9] Hammarlund K. The social impacts of wind power. In: Presented at EWEA Conference, Goteborg, Sweden; 1997.

[10] Pedersen E, Persson Waye K. The impact of wind turbines in Sweden with special reference to noise annoyance. In: Presented at EWEA Conference, Copenhagen, Denmark; 2001.
[11] Van Renterghem Timothy, Bockstael Annelies, De Weirt Valentine, Botteldooren Dick. Annoyance, detection and recognition of wind turbine noise original research article science of the total environmentVols. 456–457; 1 July 2013. p. 333–45.
[12] Lighthill MJ. On sound generated aerodynamically i. General theory. Proc R Soc Lond 1952;211(1107):564587.
[13] Lighthill MJ. On sound generated aerodynamically ii. Turbulence as a source of sound. Proc R Soc Lond 1954;222(1148):1–32.
[14] Curle N. The influence of solid boundaries upon aerodynamic sound. Proc R Soc Lond 1955;231:505–14.
[15] Ffowcs-Williams JE, Hall LH. Aerodynamic sound generation by turbulent flow in the vicinity of a scattering half plane. J Fluid Mech 1970;40(4): 657–70.
[16] Ffowcs-Williams JE, Hawkings DL. Sound generation by turbulence and surfaces in arbitrary motion. Proc Roy Soc Lond 1969;A264:321–42.
[17] Amiet RK. Acoustic radiation from and airfoil in a turbulent stream. J Sound Vib 1975;41(4):407–20.
[18] Lutz Th, Herrig A, Würz W, Kamruzzaman M, Krämer E. Design and wind-tunnel verification of low-noise airfoils for wind turbines. AIAA J 2007;45(4):779–85.
[19] Kamruzzaman M, Herrig A, Lutz W, Würz Th, Kämer E, Wagner S. Comprehensive evaluation and assessment of trailing edge noise prediction based on dedicated measurements. Noise Control Eng J 2011;59(1):54–67.
[20] Moriarty PJ, Oerlemans S. Wind tunnel aeroacoustic tests of six airfoils for use on small wind turbines. In: 42nd AIAA Aerospace Science Meeting and Exhibit; 2004.
[21] Bertagnolio F, Aa Madsen H, Bak C. Experimental validation of two trailing edge noise model and application to airfoil optimization. In: Conference Proceedings EWEC; 2009.
[22] Gömen T, özerdem B. Airfoil optimization for noise emission problem and aerodynamic performance criterion on small scale wind turbines. Orig Res Article Energy 2012;46(1):62–71.
[23] Wolsink M. Wind power implementation: the nature of public attitudes: equity and fairness instead of 'backyard motives'. Renew Sustain Energy Rev 2005:1188–207.
[24] Devine-Wright P. Beyond NIMBYism: towards an integrated framework for understanding public perceptions of wind energy. Wind Energy 2005: 125–39.
[25] Taylor Jennifer, Eastwick Carol, Lawrence Claire, Wilson Robin. Noise levels and noise perception from small and micro wind turbines. Orig Res Article Renew Energy July 2013;55:120–7.
[26] Theofiloyiannakos D, Zorlos P, Agoris D. Current practices for the prediction and assessment of the environmental impact from wind energy projects in Greece. In: Presented at EWEA Conference, Copenhagen, Denmark; 2001.
[27] Prospathopoulos JM, Voutsinas SG. Application of a ray theory model to the prediction of noise emissions from isolated wind turbines and wind parks. Wind Energy 2007:103–19.
[28] Rogers T, Omer S. The effect of turbulence on noise emissions from a micro-scale horizontal axis wind turbine. Orig Res Article Renew Energy May 2012;41:180–4.
[29] Henrik M, Christian SP. Low-frequency noise from large wind turbines. Acoustical Society of America; 2011. p. 3727–44.
[30] Van Den Berg GP. Effects of the wind profile at night on wind turbine sound. J Sound Vib 2004:955–70.
[31] Oerlemans S, Sijtsma P, Méndez López B. Location and quantification of noise sources on a wind turbine. J Sound Vib 2007:869–83.
[32] H. Dumitrescu, V. Cardoş, A. Dumitrache, F. Frunzulică, Low-frequency noise prediction of vertical axis wind turbines. Proceedings of the Romanian Academy, Series A, Vol. 11, Number 1/2010, pp. 47–54.
[33] Filios AE, Tachos NS, Fragias AP, Margaris DP. Broadband noise radiation analysis for an HAWT rotor. Renew Energy 2007:1497–510.
[34] Fluent Inc.. Fluent 6.3.26 users guide. Fluent Inc.; 2005.
[35] Brentner KS, Farassat F. An analytical comparison of the acoustic analogy and Kirchhoff formulations for moving surfaces. AIAA J 1998;36(8).
[36] Mohamed MH. Performance Investigation of H-rotor Darrieus turbine with new airfoil shapes. Energy 2012;47(1):522–30.
[37] Mohamed MH. Impacts of solidity and hybrid system in a small wind turbine performance. Energy 2013;57(8):495–504.
[38] Mohamed MH, Janiga G, Pap E, Thvenin D. Optimization of Savonius turbines using an obstacle shielding the returning blade. Renew Energy 2010;35(11): 2618–26.
[39] Mohamed MH, Janiga G, Pap E, Thvenin D. Optimal blade shape of a modified Savonius turbine using an obstacle shielding the returning blade. Energy Convers Manag 2011;52(1):236–42.
[40] Mohamed MH, Janiga G, Pap E, Thvenin D. Multi-objective optimization of the airfoil shape of wells turbine used for wave energy conversion. Energy 2011;36(1):438–46.
[41] Mohamed MH, Shapaan S. Optimization of blade pitch angle of an axial turbine used for wave energy conversion. Energy 2013;56(7):229–39.
[42] Trivellato F, Raciti Castelli M. On the courant-friedrichs-lewy criterion of rotating grids in 2d vertical-axis wind turbine analysis. Renew Energy 2014;2014(62):53–62.
[43] http://m-selig.ae.illinois.edu/ads/coord/s1046.dat. Last access August 2015.

Nomenclature

A: Projected area of rotor (DH), m^2
C_p: Power coefficient ($P/[1/2\rho AU^3]$)
c: Single blade chord, m
D: Turbine diameter ($2R$), m
H: Blade height, m
N: Rotational speed of rotor, rpm
n: Number of blades
R: Radius of turbine, m
U: Mean wind velocity in axial direction, m/s
u: Peripheral velocity of the blade, m/s
σ: Solidity, ($nc/2R$)
λ: Tip Speed Ratio (TSR), ($\omega R/U$)
ρ: Density, kg/m^3
ω: Angular speed, 1/s
u_i: Fluid velocity component in the x_i direction
u_n: Fluid velocity component normal to the surface $f = 0$
v_i: Surface velocity components in the x_i direction
v_n: Surface velocity component normal to the surface
$\delta(f)$: Dirac delta function
$H(f)$: Heaviside function
p: Sound pressure at the far field
T_{ij}: Lighthill's stress tensor
a_0: Far-field sound speed